104 (2025) 105052

Contents lists available at ScienceDirect

Poultry Science

journal homepage: www.elsevier.com/locate/psj

Full-Length Article

Deoxynivalenol-induced pyroptosis and autophagy inhibition collectively promote inflammatory injury in the glandular stomach of chicken embryos

Fu Chen [a,1], Guoming Yang [a,1], Huiling Qiu [b], Shansong Gao [a], Lele Hou [a], Jihong Dong [a], Peng Zhao [c], Wenxuan Dong [a,*]

[a] Institute of Animal Nutritional Metabolic and Poisoning Diseases, College of Veterinary Medicine, Qingdao Agricultural University, Qingdao, 266109, Shandong Province, China
[b] Haidu College, Qingdao Agricultural University, Laiyang, 265200, Shandong Province, China
[c] College of Ecology and Environment, Baotou Teachers' College, Inner Mongolia University of Science and Technology, Baotou, 014030, China

ARTICLE INFO

Keywords:
Deoxynivalenol
glandular stomach
chicken embryos
pyroptosis
autophagy

ABSTRACT

Glandular stomach plays a crucial role in the digestive system and overall physiological functions of chickens. Mycotoxins, including deoxynivalenol (DON), in contaminated feed damage the immune and digestive systems of chickens and hinder their growth. However, the mechanism underlying DON toxicity on glandular stomach inflammation remains unclear. This study found that DON induced inflammation and injury in the glandular stomach of chicken embryos by regulating pyroptosis and autophagy. DON stimulated proinflammatory factor release, activated NLRP3 inflammasome and its downstream elements, increased caspase-3 and GSDME expression to mediate pyroptosis and injury, and inhibited autophagy in glandular stomach by decreasing ATG5, ATG7, and Beclin-1 expressions and increasing mTOR expression. Besides, DON reduced LC3-II/LC3-I ratio and elevated p62 expression. These results confirmed the association between DON-induced pyroptosis and autophagy inhibition, providing key evidence for understanding DON toxicity and mitigating DON contamination in poultry farming; nevertheless, the underlying mechanism must be further elucidated.

Introduction

Deoxynivalenol (DON) is an important mycotoxin (a toxic substance produced by fungi) that poses a potential threat to public health due to its presence on staple crops such as corn, barley, and wheat on a global scale (Mishra et al., 2020, Sumarah, 2022). Since its discovery in 1974, DON has been detected in cereal-growing areas, with incidences of chronic and, at times, elevated levels of exposure in both humans and animals (Thapa et al., 2021). DON, although not being the most acutely toxic trichothecene, is widely prevalent in various cereals, and its persistence during storage and food preparation exacerbates the problem, especially in food and livestock industries (Park et al., 2018, Rotter et al., 1996). While the permissible limits for DON in diverse foodstuffs vary among different countries, the presence of DON even within these thresholds can exert cumulative and long-term impacts on public health (Thapa et al., 2021). Temperature, humidity, and precipitation have been reported to be the principal climatic determinants governing the occurrence and spread of mycotoxin-generating fungi. The increasing frequency of extreme weather phenomena, attributable to global warming in recent times, is hypothesized to have exacerbated the contamination of foodstuffs by mycotoxins, especially DON (Zingales et al., 2022). The fluctuations in the levels of DON within the primary maize-producing regions of China have effectively confirmed the influence of precipitation on DON contamination (Gruber-Dorninger et al., 2019), which may inevitably worsen the adverse effects of DON on food security (Chen et al., 2024). However, the toxicology of DON-related health issues is complex and not yet fully elucidated, and the current prevention and control strategies are inadequate. Therefore, it is imperative to undertake in vitro and in vivo research to elucidate the toxicology of DON, which could potentially facilitate the development of more effective measures to safeguard public health and reduce associated economic losses in agriculture and animal husbandry.

Feed intake is the major route through which DON enters the animal body and causes damage, emphasizing the crucial role of the digestive system in the toxicology of DON (Liang and Wang, 2023). Previous studies on the gastrointestinal damage in animals resulting from the

* Corresponding author.
E-mail address: dongwenxuan7@163.com (W. Dong).
[1] These authors contributed equally to the work.

https://doi.org/10.1016/j.psj.2025.105052
Received 20 January 2025; Accepted 15 March 2025
Available online 17 March 2025

ingestion of DON-contaminated feed have mainly focused on the intestines, and have found that DON could damage the intestinal epithelial cells, shorten the intestinal villi, and disrupt the intestinal barrier (Pinton and Oswald, 2014, Yang et al., 2019). As the first major digestive organ in the avian digestive system, glandular stomach provides the necessary components and conditions for digestion and absorption in the intestine through its chemical decomposition function. Our previous research demonstrated that DON induces glandular stomach damage by triggering the infiltration of immune cells and inflammatory responses (Hou et al., 2023), suggesting that autophagy and pyroptosis, which are closely related to the release of inflammatory cytokines, may be involved in the glandular stomach damage induced by DON. Moreover, DON can trigger and sustain inflammatory response in the glandular stomach of chicken embryos (Hou et al., 2023).

Pyroptosis is a form of inflammatory cell death that has been widely studied in recent years, and is characterized by membrane pore formation, swelling, and subsequent cell lysis, accompanied by the release of proinflammatory intracellular contents (Shi and Gao, 2017). Gasdermin D (GSDMD) and gasdermin E (GSDME) are the key proteins involved in the pathogenesis of pyroptosis. GSDME, initially identified as DFNA5, can transform caspase-3-mediated apoptosis induced by TNF or chemotherapy drugs into pyroptosis; this transformation is facilitated by the specific cleavage of GSDME by caspase-3 to generate a GSDME-N fragment that perforates membranes and induces pyroptosis (Wang et al., 2017). However, given that the vast majority of studies on pyroptosis have focused on GSDMD, further research is required to elucidate the stimuli that activate GSDME and the specific cellular functions of GSDME in inflammatory diseases (Wei et al., 2023). In the present study, autophagy inhibition and pyroptosis were found to be correlated to DON-induced inflammatory damage, and their combined effects on the toxicity of DON in the glandular stomach of chicken embryos were established. Our results may provide novel experimental and theoretical foundations for the prevention and treatment of DON-induced avian glandular gastritis.

Materials and methods

Chemicals and reagents

Chicken interleukin-1β (IL-1β) ELISA kit (ml059835), chicken tumor necrosis factor-α (TNF-α) ELISA detection kit (ml002790), chicken IL-6 ELISA kit (ml023415), and chicken nuclear factor-κB (NF-κB) ELISA kit (ml002789) were purchased from Shanghai Lianke Biotechnology Co., Ltd. (Shanghai, China). PARK2/Parkin Polyclonal antibody (14060-1-AP), ATG5 Polyclonal antibody (10181-2-AP), Caspase-1/p20/p10 Polyclonal antibody (22915-1-AP), ASC/TMS1 Polyclonal antibody (10500-1-AP), NLRP3 Polyclonal antibody (19771-1-AP), ATG7 Polyclonal antibody (10088-2-AP), PINK1 Polyclonal antibody (23274-1-AP), and DFNA5/GSDME Polyclonal antibody (13075-1-AP) were procured from Wuhan Sanying Biotechnology Co., Ltd. (Wuhan, Hubei, China). NF-κB p65 (WL01273b), Caspase-3/Cleaved Caspase-3 (WL02117), TLR4 (WL00196), Cleaved N-terminal GSDMD (WL05411), and Goat Anti-Rabbit IgG H&L/HRP (BA12163708) were purchased from Shenyang Wanlei Biotechnology Co., Ltd. (Shenyang, Liaoning, China). Rabbit Anti-phospho-NF-KB p65 (Ser536) antibody (bs-0982R) was bought from Biosynthesis Biotechnology Co., Ltd. (Beijing, Beijing, China). GAPDH Antibody (AF7021) was obtained from Jiangsu QinKe Biological Research Center Co., Ltd. (Nanjing, Jiangsu, China) and DON (51481-10-8) was purchased from Pribolab Bioengineering Co., Ltd. (Qingdao, Shandong, China). UNlQ-10 Column Trizol total RNA extraction kit (B511321) was obtained from Shanghai Sangon Biotech Co., Ltd. (Shanghai, Shanghai, China). All the other chemicals and reagents used in this study are consistent with those employed in our previous research (Hou et al., 2023).

Animals and experimental design

The protocols for obtaining chicken embryos and DON exposure treatment were in accordance with those reported in our previous study (Hou et al., 2023). The flow chart illustrating the experimental design is shown in Figure S1. In brief, a total of 250 9-day-old chicken embryos were randomly allocated into five groups, with each group consisting of five replicates of incubation trays and ten chicken embryos per tray. Different concentrations of DON (0 (control), 1.0 (L), 5.0 (M), 10.0 (H), and 20.0 μg(SH)) were injected into the allantoic cavity of the chicken embryos in the five groups. Following DON injection, the embryos were incubated under optimal temperature and humidity conditions until 10, 12, and 15 days post-injection, respectively, and samples were collected at these time points.

Histological analysis of the glandular stomach

The methods for organ index and glandular stomach histopathological analysis are consistent with those described in our previous study (Hou et al., 2023). To further quantify the pathological changes in the glandular stomach tissues, a comprehensive histological scoring system was employed. For epithelial disruption, a 0–3 scale was employed, with 0 denoting intact epithelium with no damage or detachment signs; 1 representing minor disruptions such as sporadic cell flattening or slight basal layer lifting; 2 corresponding to moderate damage with visible epithelial gaps and partial cell loss; and 3 indicating severe destruction with loss of large epithelial areas and significant cell shedding.

With regard to the degree of inflammation, a similar 0–3 scale was used. A score of 0 implied no inflammatory cells in the local tissue section; 1 indicated a few scattered lymphocytes near blood vessels; 2 denoted a moderate infiltration of neutrophils and macrophages in the lamina propria and submucosa; and 3 signified a heavy influx of inflammatory cells with widespread infiltration and potential microabscess formation in severe cases.

The extent of tissue degeneration was assessed based on 0–3 scale, with 0 representing normal tissue architecture without degeneration; 1 denoting mild degeneration such as slight cytoplasmic vacuolation; 2 indicating moderate degeneration with prominent vacuolation, nuclear pyknosis, and loss of cell polarity; and 3 representing severe degeneration with extensive necrosis and loss of tissue structure.

To ensure reliability and reproducibility, three independent and experienced pathologists performed blinded evaluations. The final pathological score for each sample was obtained by summing up the scores of epithelial disruption, degree of inflammation, and extent of tissue degeneration.

ELISA

Sample pretreatment

The glandular stomachs of chicken embryos were harvested and rinsed promptly with pre-chilled PBS (0.01 M, pH 7.4) to eliminate residual blood. About 0.1 g of tissue was weighed, minced, mixed with 0.1 mL of PBS, and thoroughly ground on ice in a 1.5-mL centrifuge tube. Subsequently, 0.8 mL of PBS was added to the mixture to form a homogenate. Then, the homogenate was centrifuged at 5000 × g for 10 min, and the supernatant was used for further assays.

ELISA

The ELISA kit was equilibrated at room temperature for 30 min according to the manufacturer's instructions. The standard wells contained 50 μL of different concentrations of standards (three replicates per group) and 100 μL of HRP-labeled detection antibody, while the sample wells comprised 50 μL of samples (three replicates per group) and 100 μL of HRP-labeled detection antibody. The wells were sealed with a cover membrane and incubated at 37°C for 60 min. After incubation, the liquid was discarded, and the wells were blotted dry on an

Table 1
The organ index of chicken embryo glandular stomach (n=5).

Day	Groups	MEAN±SD (g/kg)	P vaule
10d	CON	3.587±0.475	-
	L	3.506 ±0.368	0.782
	M	3.287 ±0.978	0.595
	H	2.975 ±0.803	0.258
	S	2.970 ±0.959	0.282
12d	CON	5.244 ±0.779	-
	L	4.131 ±0.263**	0.006
	M	4.224 ±0.237*	0.012
	H	4.119 ±0.548**	0.006
	S	4.219 ±0.393*	0.012
15d	CON	7.143 ±0.981	-
	L	7.110 ±0.973	0.948
	M	6.760 ±0.916	0.458
	H	6.238 ±0.342	0.089
	S	5.923 ±0.587*	0.026

Note: Compared with the CON group
* indicates significant difference ($p < 0.05$),
** indicates extremely significant difference ($P < 0.01$), and no * indicates no significant difference ($P > 0.05$)

absorbent paper. Then, 350 μL of washing buffer were added to each well, and after 1 min, the buffer was removed and the wells were blotted again. This washing step was repeated five times. Subsequently, 50 μL each of substrate A and B were added to each well, and the wells were incubated in the dark at 37°C for 15 min. After incubation, 50 μL of stop solution were added, and the OD values at 450 nm were measured within 15 min and the concentrations of inflammatory factors (IL-1β, IL-6, TNF-α, and NF-κB) in the glandular stomach were calculated.

qRT-PCR

The glandular stomach tissues of chicken embryos (0.1 g of tissue per sample) were treated with TRIzol (Invitrogen, Waltham, MA, USA) and reverse-transcribed into cDNA. Then, 2 μL of cDNA per well were collected to determine the relative mRNA levels using SYBR® Premix Ex Taq™ RT-PCR kit. All the assays were performed across four independent experiments, and the relative mRNA levels of the target genes were calculated using the comparative threshold cycle ($2^{-\Delta\Delta Ct}$) method. The primers used in this study are listed in Table S1.

Western blot analysis

Approximately 0.1 g of chicken embryonic glandular stomach tissue per sample was used to extract the total protein as described elsewhere (Mu et al., 2019). After extraction, protein quantification was performed using the BCA method (Solarbio, Biotechnology Beijing, China). Subsequently, the protein was separated using SDS-PAGE with 10% separation gel and 13% concentrated gel, and then transferred onto a polyvinylidene difluoride (PVDF) membrane (0.22 μm). The PVDF membrane was immersed in 5% skim milk at room temperature for 1.5 h and incubated with primary antibodies at 4°C overnight. Then, the membrane was incubated with secondary antibody for 30 min at room temperature. Finally, the blot bands were observed and analyzed using Tanon chemiluminescence imaging analysis system. The proteins were detected and quantified using Image Lab Software (Bio-Rad, USA) and Image J software, respectively, with GAPDH band serving as the control for standardized quantitative analysis.

Transcriptomic analysis of the glandular stomach

Transcriptomic analysis of the glandular stomach of chicken embryo was performed as described previously (Hou et al., 2023).

Table 2
The mortality rate of DON on chicken embryos (n=50).

Day	Groups	Totality	Number of deaths	Mortality rate
10d	CON	50	2	4%
	L	50	7	14%
	M	50	9	18%
	H	50	14	28%
	S	50	19	38%
12d	CON	50	5	10%
	L	50	8	16%
	M	50	15	30%
	H	50	16	32%
	S	50	21	42%
15d	CON	50	6	12%
	L	50	10	20%
	M	50	16	32%
	H	50	19	38%
	S	50	27	54%

Statistical analysis

The lethal dose (LD50) values and 95% confidence intervals were calculated using Koch's method. All the data were obtained from a minimum of three independent experiments, and are presented as the mean ± standard error of the mean (SEM). Homogeneity of data and significance of intergroup differences were analyzed by one-way ANOVA and LSD, respectively, using SPSS 25.0, and $P < 0.05$ was considered statistically significant.

Results

Multidimensional exploration of the effects of DON on the glandular stomach tissue of chicken embryos

To investigate the effects of DON on the glandular stomach tissue of chicken embryos, we initially determined the glandular stomach organ index and embryonic lethality rate at different DON concentrations and time points. The results showed that the glandular stomach organ index significantly declined at 12 and 15 days, presenting a dose-dependent pattern (Table 1). When compared with the control group, the embryonic lethality rate of the DON-treated groups was significantly higher. With the increase in DON concentration and reaction time, the embryonic lethality rate exhibited a progressively upward trend, indicating that DON has a pronounced negative impact on chicken embryo development and exhibits dose/time dependency (Table 2). With regard to the pathological changes in the glandular stomach tissues of chickens in different treatment groups, various degrees of alterations, such as modifications in the intermuscular space, epithelial arrangement, cell shedding, and secretions, were observed. Besides, more severe changes were detected in the glandular gastric mucosa and related structures in the higher DON concentration groups, when compared with those in the control and lower DON concentration groups (Fig. 1A-B). Analysis of the DON levels in different tissues of chicken embryos (Fig. 1C–E) indicated that the glandular stomach, intestine, muscle, brain, and liver tissues exhibited higher DON content in a dose-dependent manner, when compared with those in the control; however, no significant variations were found in the DON content in the gizzard and heart. Correlation analysis demonstrated that the DON content in the glandular stomach was positively correlated with that in the intestine, muscle, brain, liver, and gizzard tissues, but had no significant correlation with that in the heart tissue (Fig. 1F).

Effect of DON on the secretion of proinflammatory factors in chicken embryo allantoic fluid

Following DON injection, the cytokines in the allantoic fluid of chicken embryos exhibited a complex variation profile, which was

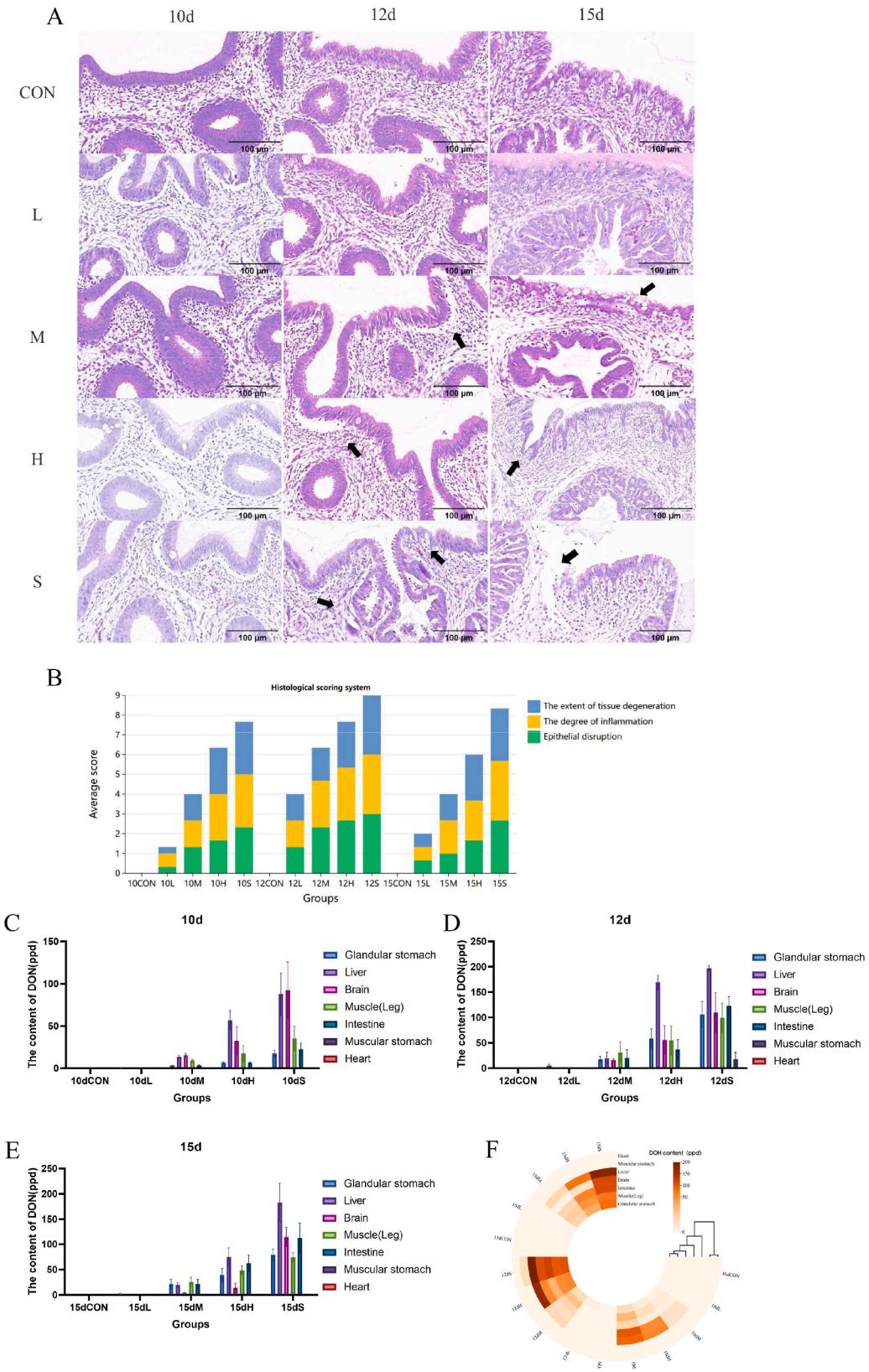

Fig. 1. Multidimensional exploration of the impact of DON on the glandular stomach tissue of chicken embryos. (A) HE staining of chicken embryos exposed to different DON concentrations and incubation periods (black arrow indicates the location of the damage). (B) HE stained pathological sections scoring results. (C–F) ELISA of the DON content in organs, including glandular stomach, liver, brain, muscle (leg), intestine, muscular stomach, and heart of chicken embryos exposed to different DON concentrations and incubation periods (n=3).

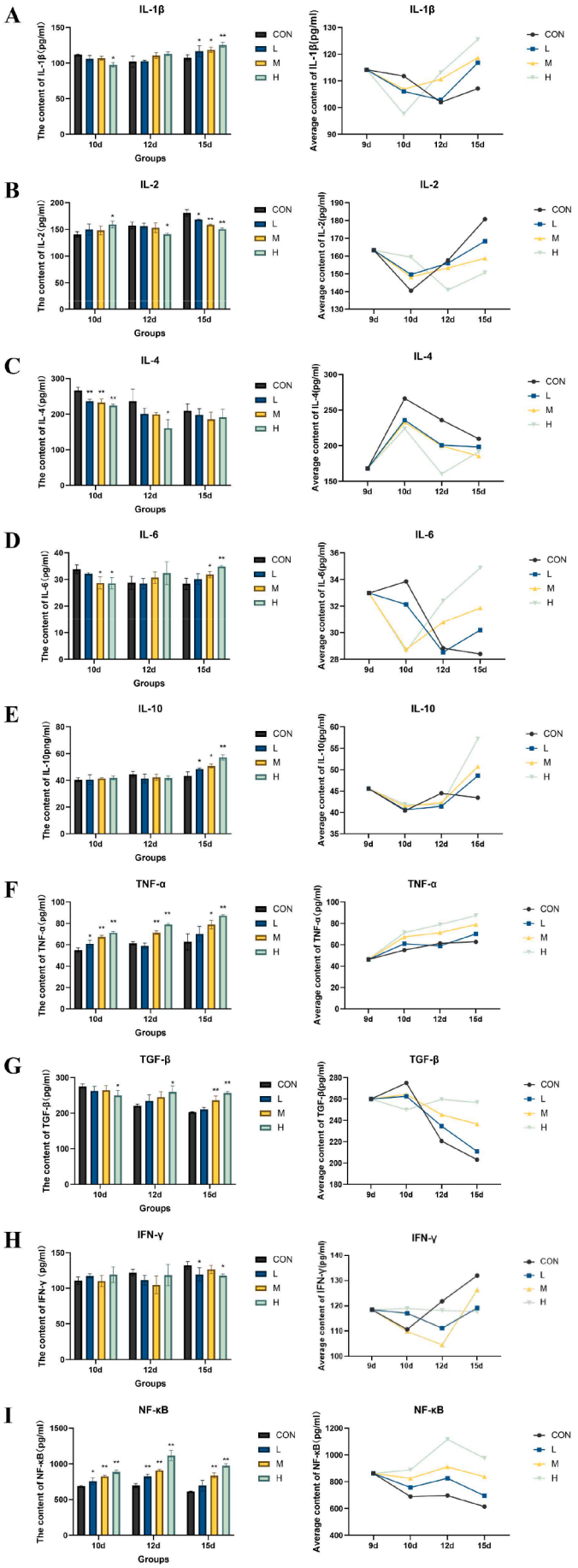

(caption on next column)

Fig. 2. Effects of DON on the secretion of proinflammatory factors in chicken embryo allantoic fluid. (A–I) ELISA of the contents of inflammatory factors, including IL-1β, IL-2, IL-4, IL-6, IL-10, TNF-α, TGF-β, IFN-γ, and NF-κB in the chicken embryo allantoic fluid exposed to different DON concentration and incubation periods (n=3). Note: When compared with the CON group, * indicates significant difference ($P < 0.05$), ** denotes extremely significant difference ($P < 0.01$), and absence of * indicates no significant difference ($P > 0.05$).

strongly correlated with the DON concentration and incubation period (Fig. 2A–I). In the low DON concentration group (L group, 1.0 μg), the IL-4 level in the allantoic fluid was significantly decreased ($P < 0.05$), whereas the TNF-α and NF-κB levels were markedly elevated ($P < 0.05$) at 10 days post-injection, when compared with those in the control group; however, at 12 days post-injection, only the NF-κB level was significantly increased ($P < 0.05$), and at 15 days post-injection, the IL-2 level was evidently reduced ($P < 0.05$), while the IL-10 level was substantially increased ($P < 0.05$) in the L group. Overall, with the progression of the incubation period, the IL-1β, IL-2, and IL-10 levels generally exhibited a pattern of initial decline followed by an increase; the IL-4 and TGF-β levels primarily showed an initial increase and subsequent decrease; the TNF-α level tended to increase; the NF-κB level initially decreased and then increased; and the IL-6 level decreased first and then increased in the L group.

In the higher DON concentration groups (M 5.0 μg and H 10.0 μg groups), the TNF-α and NF-κB levels were significantly increased ($P < 0.05$) in the M group, while the IL-1β, IL-4, and IL-6 levels were significantly decreased ($P < 0.05$) and the TNF-α, TGF-β, and NF-κB levels were significantly increased ($P < 0.05$) in the H group at 10 days post-injection. When compared with the L group, the TNF-α and NF-κB levels were significantly increased ($P < 0.05$) in the M group, while the IL-1β level was significantly reduced ($P < 0.05$) and the TNF-α and NF-κB levels were significantly increased ($P < 0.05$) in the H group. When compared with the M group, the IL-1β level was significantly lower ($P < 0.05$), whereas the NF-κB level was significantly higher ($P < 0.05$) in the H group. At 12 days post-injection, the IL-4 and IL-6 levels were significantly reduced ($P < 0.05$) in the M group, whereas the TNF-α, TGF-β, and NF-κB levels were significantly increased ($P < 0.05$) and the IL-2 level was significantly decreased ($P < 0.05$) in the H group. In addition, when compared with the L group, the TNF-α and NF-κB levels were significantly increased ($P < 0.05$) in the M group, whereas the IL-2 and IL-4 levels were significantly decreased ($P < 0.05$) and the IL-1β, TNF-α, and NF-κB levels were significantly enhanced ($P < 0.05$) in the H group. When compared with the M group, the IL-2 and IL-4 levels were more evidently decreased ($P < 0.05$), while the TNF-α and NF-κB levels were significantly increased ($P < 0.05$) in the H group. At 15 days post-injection, the IL-1β, IL-10, TNF-α, TGF-β, and NF-κB levels were significantly increased ($P < 0.05$) and the IL-2 level was significantly decreased ($P < 0.05$) in the M group; whereas the IL-2 level was significantly reduced ($P < 0.05$) and the IL-1β, IL-6, IL-10, TNF-α, TGF-β, and NF-κB levels were significantly increased ($P < 0.05$) in the H group. When compared with the L group, the IL-2 level was evidently decreased ($P < 0.05$) and the TGF-β and NF-κB levels were significantly increased ($P < 0.05$) in the M group, whereas the IL-2 level was significantly decreased ($P < 0.05$) and the IL-6, IL-10, TNF-α, TGF-β, and NF-κB levels were significantly increased ($P < 0.05$) in the H group. When compared with the M group, the IL-2 level was markedly decreased ($P < 0.05$) and the IL-10, TGF-β, and NF-κB levels were significantly increased ($P < 0.05$) in the H group. It must be noted that throughout the experimental process, the IL-10 and IFN-γ levels in the allantoic fluid of each group mostly remained relatively stable ($P > 0.05$). In particular, at the crucial time point of 12 days post-injection, the L, M, and H groups presented rather prominent cytokine variation characteristics. For instance, the NF-κB level notably increased in the L group, the IL-4 and IL-6 levels decreased and the TNF-α and NF-κB levels increased in the M group, and

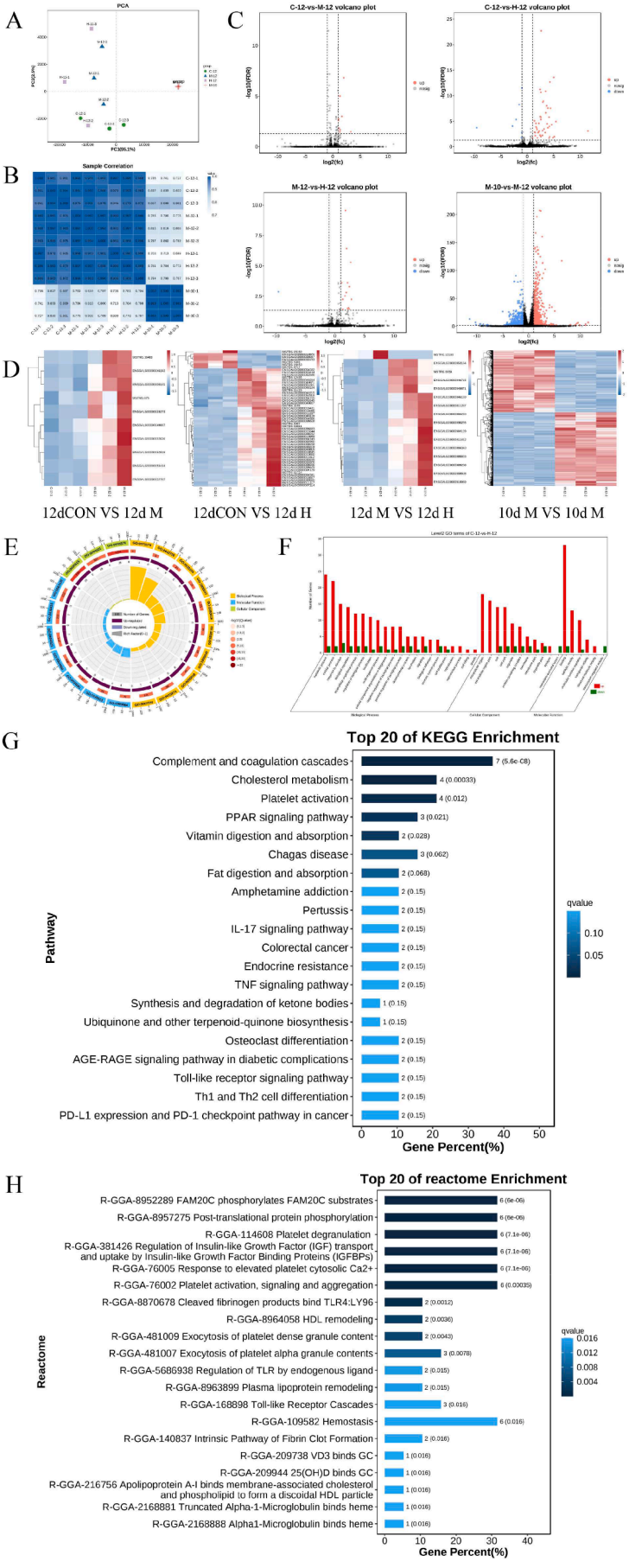

(caption on next page)

Fig. 3. Transcriptomic analysis results of the glandular stomach of chicken embryos exposed to DON (n=3). (A) PCA results of the gene expression levels in the glandular stomach of the 12dCON, 12dM, 12dH, and 10dM groups. (B) Heatmap of correlation analysis between two samples. (C) Volcanic map of DEGs between two groups. (D) Heatmap of hierarchical clustering of differential gene expression patterns compared between two groups. (E) GO enrichment circle comparison between the 12dCON and 12dH groups. (F) GO enrichment classification bar chart for comparison between the 12dCON and 12dH groups (red indicates increase and green denotes decrease). (G) KEGG enrichment bar chart comparing the 12dCON and 12dH groups. (H) Reactome enrichment bar chart comparing the 12dCON and 12dH groups.

the IL-2 level decreased and the TNF-α, TGF-β, and NF-κB levels increased in the H group. Moreover, the differences between the M and H groups were also distinct at 12 days post-injection. These alterations not only reflected the substantial impact of DON on the immunoregulation of chicken embryos at 12 days post DON exposure, but also suggested that 12 days might be a critical time point in the DON-induced immune response process in chicken embryos.

Transcriptomic analysis of the effects of DON exposure on chicken embryonic glandular stomach

Transcriptomic analyses were performed using the glandular stomach samples from the control, M, and H groups collected at 12 days post-injection (12dCON, 12dM, and 12dH groups, respectively; n = 3). The principal component analysis (PCA) results (Fig. 3A) demonstrated that the 12dCON and 12dH groups had a greater genetic distance in the PCA plot, when compared with the 12dCON and 12dM groups, indicating substantial differences in gene composition. The correlation heatmap (Fig. 3B) exhibited good repeatability among intra-group replicates. The differential comparison volcano plot (Fig. 3C) revealed significant gene differences between the 12dCON and 12dH groups, with 53 differentially expressed genes (DEGs) (46 upregulated and 7 downregulated); between the 12dM and 12dH groups, with 16 DEGs (15 upregulated and 1 downregulated); and between the 12dCON and 12dM groups, with 10 upregulated DEGs. The differential gene clustering heatmap (Fig. 3D) further indicated a considerable genetic disparity between the 12dCON and 12dH groups. Therefore, we performed inter-group comparison of the 12dCON and 12dH groups. The GO enrichment analysis (Fig. 3E and F) showed 21 upregulated and 16 downregulated genes in molecular function, 10 upregulated and 8 downregulated genes in cellular component, and 5 upregulated and 3 downregulated genes in biological process. The differential KEGG enrichment analysis (Fig. 3G) between the 12dCON and 12dH groups revealed that the upregulated DEGs were mainly enriched in pathways such as complement and coagulation cascade, cholesterol metabolism, platelet activation, PPAR, vitamin digestion and absorption, and several disease and signaling pathways. Reactome enrichment analysis (Fig. 3H) demonstrated that the upregulated DEGs were predominantly enriched in pathways related to platelet functions, TLR interactions, lipoprotein remodeling, and hemostasis.

Changes in pyroptosis-related indices in the chicken embryonic glandular stomach after DON exposure

To determine the underlying mechanism of DON-induced pyroptosis, the content of inflammatory cytokines within the glandular stomach tissues of chicken embryos was quantified. As illustrated in Fig. 4A–D, when compared with the control, a significant increase in the IL-6, IL-1β, NF-κB, and TNF-α levels was observed in the DON-treated groups. The qRT-PCR results revealed that exposure to high concentration of DON led to an evident increase in the transcriptional abundances of proinflammatory factors such as IL-6, IL-18, TNF-α, NF-κB, P38, PPARA, STING, and cGAS in the glandular stomach tissues. In contrast, exposure to low concentrations of DON either led to no substantial alteration or a decrease in the transcriptional abundances of proinflammatory factors (Fig. 4E–L). Concurrently, DON exposure caused a significant upregulation in the transcriptional levels of pyroptosis-related factors, such as CASP1, CASP3, and GSDME. In addition, the transcriptional level of NLRP3 was also increased, but was not statistically significant (Fig. 4M–P). Subsequently, the expression levels of pyroptosis-related proteins in the glandular stomach were examined (Fig. 4Q–X). When compared with the control group, the protein contents of NLRP3, TLR4, GSDME, p-NF-κB, Cleaved-CASP1, and Cleaved-CASP3 in DON-treated groups were markedly enhanced in a dose-dependent manner, whereas the variation in the N-terminal of GSDMD was not prominent. These results suggested a close association between DON-induced pyroptosis and the mechanism underlying glandular stomach injury.

DON inhibited autophagy of chicken embryonic glandular stomach cells

As the effect of DON on autophagy, a dynamic recycling pathway, is complex, we examined the transcriptional levels of key genes involved in autophagy-related pathway. The qRT-PCR results (Fig. 5A–D) showed that DON exposure increased the transcriptional level of mTOR, but significantly decreased the transcriptional levels of ATG5, ATG7, and Beclin1, when compared with those in the control group, indicating that DON prevents the formation of autophagy initiation complex. Furthermore, DON reduced the LC3-II/LC3-I value and increased the SQSTM1 transcriptional level (Fig. 5E and F), suggesting that DON exposure inhibits autophagosome formation and impairs autophagic flux. Similar results were also obtained in western blot analysis (Fig. 5I–P). DON exposure increased the expression levels of p-mTOR/mTOR ratio and p62, decreased the expression levels of ATG5 and ATG7, and reduced the LC3-II/GAPDH ratio. These findings suggested that DON inhibits autophagy of the chicken embryonic glandular stomach cells. Interestingly, DON activated PINK1 and Parkin, the key initiators of mitophagy, indicating mitochondrial damage; however, this impairment was not sufficient to reverse the inhibition of autophagy caused by DON exposure (Fig. 5G and H).

Correlation analysis

Correlation analysis was employed to further verify the relationships among DON concentration, inflammation, pyroptosis, and autophagy in the glandular stomach tissues of chicken embryos. As depicted in Fig. 6, a significant positive correlation was noted between the DON concentration and the levels of inflammation-related genes (TNF-α, IL-6, IL-18, and IL-1β), pyroptosis-related genes (NLRP3, TLR4, GSDME, p-NF-κB, Cleaved-CASP1, and Cleaved-CASP3), and autophagy-related genes (mTOR, p62, PINK1, Parkin). Conversely, the DON concentration exhibited a significant negative correlation with some autophagy-related genes such as LC3, Atg5, ATG7, and Beclin-1.

Discussion

The chicken glandular stomach is a crucial organ of the digestive system, with profound implications for the entire organism. It functions as an efficient processing factory, performing the initial digestion and processing of food, and secretes digestive enzymes and gastric acid for chemical digestion, achieving physical digestion through peristaltic agitation (Mu et al., 2019). The primary role of the glandular stomach is to facilitate the process of subsequent digestion and absorption, and disruptions in its function can impede the process of digestion and cause deficiency in nutrient uptake, consequently leading to systemic metabolic disorders and immune imbalances, and affecting the growth, production performance, and disease resistance of chickens (Madkour

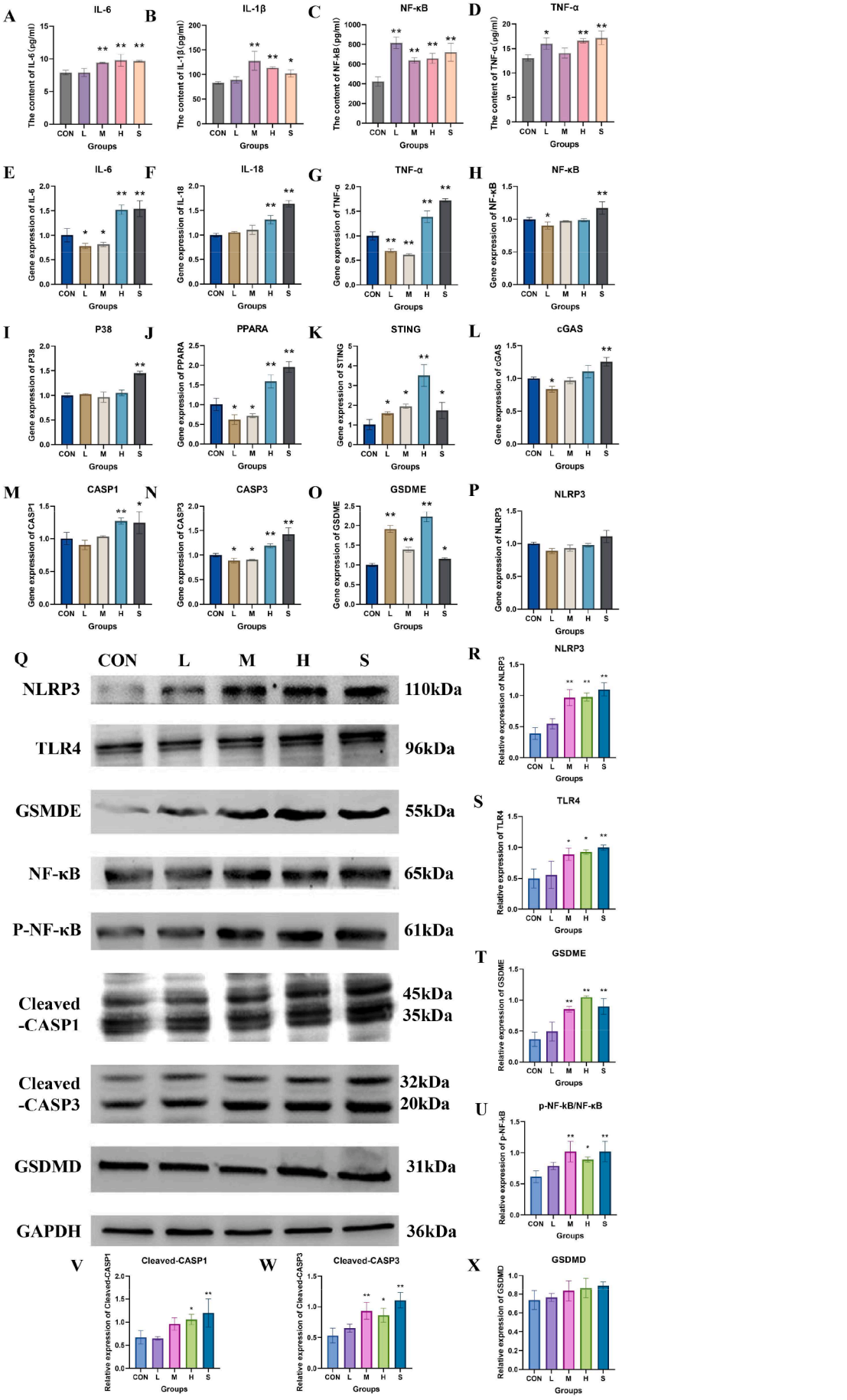

(caption on next page)

Fig. 4. Changes in pyroptosis-related indices in chicken embryonic glandular stomach after exposure to DON. (A–D) ELISA of the contents of inflammatory cytokines, including IL-6, IL-1β, NF-κB, and TNF-α in the glandular stomach. (E–P) qRT-PCR of gene expression in glandular stomach. (Q) Characteristic bands of pyroptosis-related proteins, including NLRP3, TLR4, GSDME, NF-κB, p-NF-κB, Cleaved-CASP1, Cleaved-CASP3, and GSDMD. (R–X) Statistical data for protein expression level. Note: When compared with the CON group, * indicates significant difference ($P < 0.05$), ** denotes extremely significant difference ($P < 0.01$), and absence of * indicates no significant difference ($P > 0.05$).

and Mohamed, 2019). Thus, the health and stability of the glandular stomach are extremely critical for maintaining the life activities and homeostasis of chickens.

Mycotoxins, which are toxic secondary metabolites produced by molds or fungi, exhibit rich and diverse variety, including aflatoxins, ochratoxins, zearalenone, DON, etc. They widely occur in the natural environment and tend to grow on agricultural products and feed raw materials, and produce toxins under humid and warm conditions, posing a potential health hazard to animals and humans. Besides, mycotoxins can produce adverse effects such as immunosuppression, growth retardation, and reproductive disorders. In particular, DON primarily enters into the animal body through ingestion of contaminated feed and can cause toxic damage to various physiological systems, including the immune system, digestive system, and overall growth performance (Yao and Long, 2020). Such toxic damage can trigger a series of complex pathophysiological responses in the animal body, severely affecting its health and productivity (Hou et al., 2023, Kubena et al., 1988). Previous studies on mycotoxins, especially DON, have demonstrated its high toxicity to chicken embryos, exerting diverse effects on growth and development, hematological indices, pathological changes in the glandular stomach, immunoregulation, and inflammation-related pathways (Shi and Gao, 2017). However, the specific mechanism by which DON induces inflammation in the glandular stomach of chicken embryos remains unclear.

The present study is the first to determine the ability of DON to induce inflammation and inflammatory injury in the chicken embryonic glandular stomach cells through regulation of pyroptosis and autophagy. Despite the observed variations in the extent of pyroptosis and autophagy inhibition elicited by DON exposure at different time points and DON concentrations, a distinct dose-dependent pattern was generally observed. In recent years, extensive research has been conducted to elucidate the biological effects of DON, encompassing a variety of experimental paradigms, including contamination of poultry feed, growth and development of poultry, immunomodulatory processes, and pathologies of the poultry digestive system. Both the proinflammatory and immunosuppressive properties of DON have the potential to aggravate its deleterious effects on the poultry husbandry industry, thereby impacting the growth, reproductive capacity, and disease resistance of poultry, which has consequently attracted extensive academic attention and in-depth investigations in the domain of poultry production and health (Ghareeb et al., 2015, Awad et al., 2013). Besides, DON has been observed to stimulate chronic inflammatory states or acute inflammatory surges, triggering gastrointestinal inflammation (Hooft and Bureau, 2021), hepatitis (Zong et al., 2023), cutaneous inflammation (Mishra et al., 2014), and other inflammatory maladies in diverse cell lines and animal models, concomitantly disturbing the immune function. Although poultry exhibit a relatively enhanced tolerance to DON when compared with swine, empirical investigations have confirmed that DON can attenuate the titer of infectious bronchitis virus, diminish the level of alanine aminotransferase, augment the concentration of serum cholesterol and circulating triglycerides, disrupt the humoral immune response to viral vaccines, and affect serum clinical biochemistry (Ghareeb et al., 2016). In addition, DON can compromise the functional and structural integrity of the intestine, disturbing the intestinal microbiota and ultimately causing a conspicuous decline in the productivity of broiler chickens (Wan et al., 2022, Azizi et al., 2021). Moreover, DON can induce a reduction in the intake of dry matter, calcium, and phosphorus in chickens, resulting in a decrease in body and leg weights, and its effect on the density and composition of the tibia is more pronounced than that on the femur (Keci et al., 2019). The serum phosphorus concentration demonstrated a linear decrease with the increase in the DON level, thereby deteriorating bone mineralization and disrupting mineral homeostasis in chickens. Thus, as a mycotoxin ubiquitous in the natural environment, DON can enter chickens via ingestion of contaminated feed and cause potential toxicity hazards, affecting various physiological systems in chickens, including the immune system, digestive system, and overall growth performance, thereby generating a plethora of adverse consequences and threatening poultry farming and health preservation. Accordingly, the present study aimed to determine the specific mechanism underlying DON-induced pyroptosis and autophagy inhibition.

Pyroptosis, a proinflammatory modality of cell death, is dependent on the activity of the caspase family of proteases. In particular, activated caspases cleave GSDMD to produce an N-terminal domain that plays a pivotal role in mediating pyroptosis (Shi et al., 2015). Similar N-terminal cytotoxic domain has also been noted in several other members of the gasdermin family, along with gasdermin-like proteins, such as GSDMA, GSDMB, GSDMC, and GSDME. This N-terminal region is capable of accomplishing membrane perforation, thereby facilitating pyroptosis (Wang et al., 2017, Ding et al., 2016). Interestingly, our investigations revealed that both GSDMD and GSDME are expressed in the glandular stomach of chicken embryos. Moreover, it has been reported that numerous mycotoxins have the ability to activate NLRP3, a crucial receptor associated with sterile inflammation, across diverse cell lines and tissues (Liao et al., 2024). Accordingly, we aimed to explore the role of pyroptosis in DON-induced inflammatory damage to the glandular stomach of chicken embryos. Previous studies have confirmed the diverse effects of DON on cells. In the endometrial epithelial cells of donkeys, co-incubation with DON increased the expression of caspase-1 and GSDMD (Song et al., 2022). Moreover, DON has been shown to upregulate IL-1β in mouse BV2 microglial cells and facilitate the activation of the NF-κB/ASC/NLRP3 axis (Molagoda et al., 2019). In both carp spleen lymphocytes and human keratinocytes (HaCaT cells), DON exposure led to activation of the NF-κB/NLRP3 axis that caused excessive production of mitochondrial reactive oxygen species (mtROS), disruption of mitochondrial homeostasis, and ultimately pyroptosis (Diao et al., 2024, Chen et al., 2024). Notably, Roger et al. identified a novel mechanism through which GSDME activates caspase-3 to modulate and mediate pyroptosis (Rogers et al., 2017). Exposure of HepaRG cells to 32 or 64 μM DON for 24 h produced the characteristic features of pyroptosis, such as release of IL-1β and IL-6, along with activation of caspase-3 and GSDME (Mao et al., 2022). Besides, in vivo studies found that chronic and subacute oral administration of DON caused inflammatory damage to the liver and intestine of mice by activating caspase-3/GSDME-dependent pyroptosis (Mao et al., 2023, Lu et al., 2024). However, reports on pyroptosis induced by DON in poultry are rather scarce. The findings of the present study indicated that DON can promote the release of proinflammatory factors and trigger the activation of NLRP3 and its downstream elements. However, no significant alteration was observed in the N-terminal domain of GSDMD. Furthermore, DON exposure caused significant upregulation of the expressions of caspase-3 and GSDME, which, in turn, facilitated pyroptosis and produced inflammatory damage. In the field of poultry health research, besides mycotoxins, pollutants such as microplastics can also amplify the chain of stress-inflammasome activation-pyrodeath-inflammation, causing damage to poultry lungs (Kowalska et al., 2022). This finding highlights the commonalities and differences in the mechanism of action of different harmful substances, thereby broadening the scope of

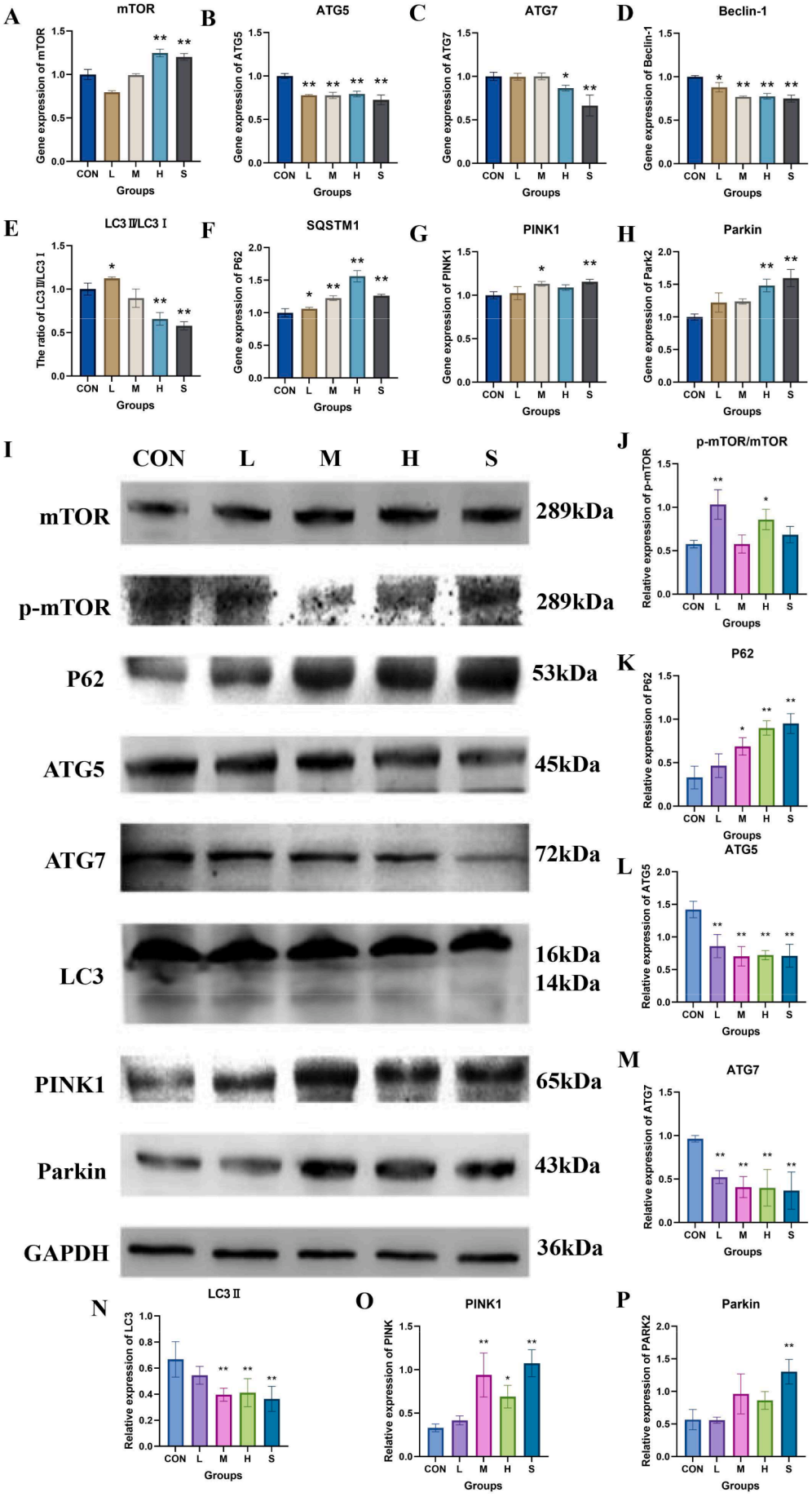

(caption on next page)

Fig. 5. DON inhibited autophagy of chicken embryonic glandular stomach cells. (A–H) qRT-PCR of gene expression in glandular stomach. (I) Characteristic bands of autophagy-related proteins, including mTOR, p-mTOR, p62, ATG5, ATG7, LC3, PINK1, and Parkin. (J–P) Statistical data for protein expression level. Note: When compared with the CON group, * indicates significant difference ($P < 0.05$), ** denotes extremely significant difference ($P < 0.01$), and absence of * indicates no significant difference ($P > 0.05$).

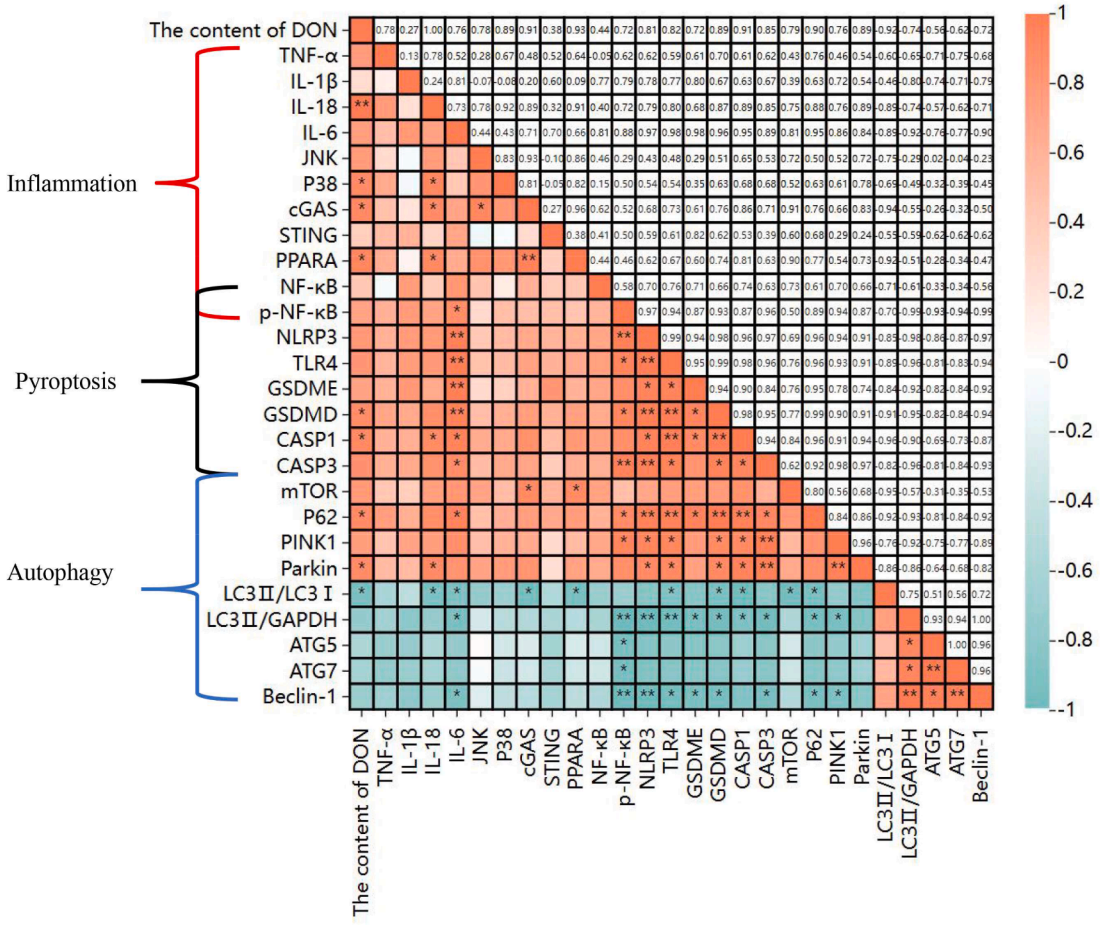

Fig. 6. Correlation analysis of inflammation, pyroptosis, and autophagy in chicken embryonic glandular stomach exposed to DON. Note: * indicates significant correlation ($P < 0.05$), ** denotes extremely significant correlation ($P < 0.01$), and absence of * indicates no significant correlation ($P > 0.05$).

research initiatives that explore the overall defense mechanisms of poultry in the face of multiple environmental threats.

Autophagy is a complex and highly regulated multistep biological process that is essential for maintaining intracellular equilibrium (Song et al., 2017). It involves the sequestration, transportation, and degradation of cytoplasmic components, including damaged organelles and misfolded proteins, through fusion with lysosomes, thereby facilitating recycling of cellular materials and energy, and has a profound influence on inflammation. As various intracellular elements, such as microorganisms, malfunctioning organelles, protein aggregates, and both organic and inorganic crystals, can act as triggers for inflammatory signals (PAMPs and DAMPs), the autophagy-mediated cytoplasmic clearance mechanism inherently exhibits anti-inflammatory property in all cell types and is capable of initiating cell-autonomous inflammatory responses (Deretic and Levine, 2018, Deretic, 2021). It has been reported that DON can induce alterations in autophagic states across multiple tissues and cell types, including human prostate epithelial cells (Kowalska et al., 2022), rat adrenal gland cells (PC12) (Wang et al., 2020), pig spleen lymphocytes (Ren et al., 2020), porcine intestinal epithelial cells (Tang et al., 2015), and murine skin (Mishra et al., 2014). Although autophagy plays a critical role in resisting DON and exhibits close association with inflammatory pathways, research on autophagy in poultry exposed to DON is scarce. In the present study, inhibition of autophagy in the glandular stomach of chicken embryos was found to be correlated with a marked decrease in the transcriptional and protein expression levels of ATG5, ATG7, and Beclin 1, accompanied by a significant increase in the mTOR level. This finding implied that DON blocks the formation of the autophagy initiation complex. Concurrently, DON decreased the LC3-II/LC3-I ratio and enhanced the p62 level, thereby corroborating that DON can reduce the formation of autophagosomes and impair autophagic flux. Interestingly, although DON activated PINK1 and Parkin, the key initiators of mitophagy, this activation failed to reverse the damage inflicted by DON on the glandular stomach. This disparity in the results could be attributed to the species-specific characteristics and exposure duration and dosage of DON (Chen et al., 2024).

Numerous studies have confirmed that the absence or impairment of autophagy can cause aberrant inflammasome activation (Takahama et al., 2018), which is correlated with an increase in caspase-1 activity and over-release of IL-1α, IL-1β, and IL-18. Autophagy can eliminate large protein complexes, exemplified by active inflammasomes. The inflammasome constituent ASC can interact with p62, and polyubiquitination of active inflammasomes expedites their transport to autophagosomes and subsequent degradation within lysosomes.

Functional data have revealed that autophagic modulation can affect inflammasome activation and release of associated cytokines (Harris et al., 2017). Moreover, autophagy has been found to exert a negative regulatory effect on the early-stage interactions of inflammasomes (Harris et al., 2017). In the dextran sulfate sodium induced colitis model, Atg16l1-deficient mice exhibited increased weight loss, exacerbated intestinal inflammation, and enhanced serum levels of IL-1β and IL-6 (Saitoh et al., 2008). Preliminary studies have demonstrated that the autophagic process can limit the production of IL-1β through a p62-dependent mechanism involving degradation of inflammasomes and their components (Shi et al., 2012). Besides, NLRP3 can participate in autophagy-correlated inflammatory modulation via a p62-dependent pathway. In addition to DON, other environmental pollutants (acetochlor) have similar effects on poultry organs, and dietary intervention methods (Omega-3) have been posited as potential protective measure (Zhang et al., 2024). These findings revealed an association between DON-induced pyroptosis and autophagy inhibition; however, the precise and intricate mechanism underlying this relationship must be further elucidated. Overall, a comprehensive understanding of the complex relationship among autophagy, inflammasomes, and DON-induced effects is crucial for determining the pathogenesis of related diseases and developing potential therapeutic strategies.

This study focused on the effects of DON on the glandular stomach of chicken embryos, which is a critical organ of the digestive system. The results revealed that DON can promote inflammation and inflammatory damage to the glandular stomach of chicken embryos by regulating pyroptosis and autophagy. The extents of pyroptosis and autophagy inhibition caused by DON exposure varied at different time points and DON concentrations, but exhibited a dose-dependent effect. Furthermore, DON induced the release of proinflammatory factors, activated NLRP3 and its downstream elements, and significantly increased the expression of caspase-3 and GSDME, which mediate pyroptosis and inflammatory damage. These results expand our understanding of the cytotoxic mechanism of DON. Furthermore, DON-induced autophagy inhibition in the glandular stomach of chicken embryos was related to the changes in a variety of autophagy-related factors, and although the key initiators of mitochondrial autophagy were activated by DON, they did not reverse the damage. Nevertheless, while a correlation between DON-induced pyroptosis and autophagy inhibition was noted, the exact mechanism remains to be further explored. In summary, these findings provide crucial evidence for a comprehensive understanding of the toxic mechanism of DON in the glandular stomach of chicken embryos, and for addressing the hazard of DON contamination in poultry farming.

CRediT authorship contribution statement

Fu Chen: Conceptualization, Investigation, Formal analysis, Data curation, Writing – review & editing. **Guoming Yang:** Conceptualization, Methodology, Data curation. **Huiling Qiu:** Software, Resources, Methodology. **Shansong Gao:** Software, Resources, Methodology, Formal analysis. **Lele Hou:** Supervision. **Jihong Dong:** Supervision. **Peng Zhao:** Supervision, Project administration, Funding acquisition. **Wenxuan Dong:** Writing – review & editing, Project administration, Conceptualization, Funding acquisition, Methodology.

Declaration of competing interest

The authors declare that they have no known competing financial interests or personal relationships that could have appeared to influence the work reported in this paper.

Acknowledgements

This work was financially supported by the Chinese National Natural Science Foundation (32373078), Shandong Natural Science Foundation (ZR2021MC150), Shandong Poultry Technology and Industry System, China (SDAIT-11-07), Inner Mongolia Autonomous Region Chinese Traditional Medicinal Crops Modern Agriculture and Animal Husbandry Industry Technology System, and Qingdao Natural Science Foundation (24-4-4-zrjj-37-jch).

Ethics Approval and Consent to Participate: Every procedure and protocol involving animals were permitted by the Qingdao Agricultural University Comparative Medical Center (Shandong Province, China). The study was based on the Guide to moral Control and Supervision in Animal Conservation and use.

The manuscript was edited for the English language, grammar, punctuation, spelling, and overall style by one or more of the highly qualified native English-speaking editors at International Science Editing (ht tp://w ww.internationalscienceediting.com).

Supplementary materials

Supplementary material associated with this article can be found, in the online version, at doi:10.1016/j.psj.2025.105052.

References

Awad, W., et al., 2013. The toxicological impacts of the fusarium mycotoxin, deoxynivalenol, in poultry flocks with special reference to immunotoxicity. Toxins. (Basel) 5, 912–925.
Azizi, T., et al., 2021. The impact of deoxynivalenol contaminated diet on performance, immune response, intestine morphology and jejunal gene expression in broiler chicken. Toxicon. 199, 72–78.
Chen, H., et al., 2024. Low-dose deoxynivalenol exposure inhibits hepatic mitophagy and hesperidin reverses this phenomenon by activating SIRT1. J. Hazard. Mater. 468, 133854.
Chen, J., et al., 2024. Chlorogenic acid attenuates deoxynivalenol-induced apoptosis and pyroptosis in human keratinocytes via activating Nrf2/HO-1 and inhibiting MAPK/NF-kappaB/NLRP3 pathways. Biomed. PharmacOther 170, 116003.
Deretic, V., 2021. Autophagy in inflammation, infection, and immunometabolism. Immunity. 54, 437–453.
Deretic, V., Levine, B., 2018. Autophagy balances inflammation in innate immunity. Autophagy. 14, 243–251.
Diao, L., et al., 2024. New insights into micro-algal astaxanthin's effect on deoxynivalenol-induced spleen lymphocytes pyroptosis in Cyprinus carpio: involving mitophagy and mtROS-NF-kappaB-dependent NLRP3 inflammasome. Fish. Shellfish. Immunol. 144, 109259.
Ding, J., et al., 2016. Pore-forming activity and structural autoinhibition of the gasdermin family. Nature 535, 111–116.
Ghareeb, K., et al., 2015. Impacts of the feed contaminant deoxynivalenol on the intestine of monogastric animals: poultry and swine. J. Appl. Toxicol. 35, 327–337.
Ghareeb, K., et al., 2016. Deoxynivalenol in chicken feed alters the vaccinal immune response and clinical biochemical serum parameters but not the intestinal and carcass characteristics. J. Anim. Physiol. Anim. Nutr. (Berl) 100, 53–60.
Gruber-Dorninger, C., Jenkins, T., Schatzmayr, G., 2019. Global mycotoxin occurrence in feed: A ten-year survey. Toxins. (Basel) 11.
Harris, J., et al., 2017. Autophagy and inflammasomes. Mol. Immunol. 86, 10–15.
Hooft, J.M., Bureau, D.P., 2021. Deoxynivalenol: mechanisms of action and its effects on various terrestrial and aquatic species. Food Chem. Toxicol. 157, 112616.
Hou, L., et al., 2023. Effect of deoxynivalenol on inflammatory injury on the glandular stomach in chick embryos. Poult. Sci. 102, 102870.
Keci, M., et al., 2019. Deoxynivalenol in the diet impairs bone mineralization in broiler chickens. Toxins. 11.
Kowalska, K., et al., 2022. Deoxynivalenol induces apoptosis and autophagy in human prostate epithelial cells via PI3K/Akt signaling pathway. Arch. Toxicol. 96, 231–241.
Kubena, L.F., et al., 1988. Influence of ochratoxin A and deoxynivalenol on growing broiler chicks. Poult. Sci. 67, 253–260.
Liang, S.J., Wang, X.Q., 2023. Deoxynivalenol induces intestinal injury: insights from oxidative stress and intestinal stem cells. Environ. Sci. Pollut. Res. Int. 30, 48676–48685.
Liao, C., et al., 2024. The novel role of the NLRP3 inflammasome in mycotoxin-induced toxicological mechanisms. Vet. Sci. 11.
Lu, H., et al., 2024. Endoplasmic reticulum stress-induced NLRP3 inflammasome activation as a novel mechanism of polystyrene microplastics (PS-MPs)-induced pulmonary inflammation in chickens. J. Zhejiang. Univ. Sci. B 25, 233–243.
Madkour, F.A., Mohamed, A.A., 2019. Comparative anatomical studies on the glandular stomach of the rock pigeon (Columba livia targia) and the Egyptian laughing dove (Streptopelia senegalensis aegyptiaca). Anat. Histol. Embryol. 48, 53–63.
Mao, X., et al., 2022. Deoxynivalenol induces caspase-3/GSDME-dependent pyroptosis and inflammation in mouse liver and HepaRG cells. Arch. Toxicol. 96, 3091–3112.
Mao, X., et al., 2023. The combined effect of deoxynivalenol and fumonisin B(1) on small intestinal inflammation mediated by pyroptosis in vivo and in vitro. Toxicol. Lett. 372, 25–35.
Mishra, S., et al., 2014. Deoxynivalenol induced mouse skin cell proliferation and inflammation via MAPK pathway. Toxicol. Appl. Pharmacol. 279, 186–197.

Mishra, S., et al., 2020. Global occurrence of deoxynivalenol in food commodities and exposure risk assessment in humans in the last decade: a survey. Crit. Rev. Food Sci. Nutr. 60, 1346–1374.
Molagoda, I., et al., 2019. Deoxynivalenol enhances IL-1ss expression in BV2 microglial cells through activation of the NF-κb pathway and the ASC/NLRP3 inflammasome. EXCLI. J. 18, 356–369.
Mu, M., et al., 2019. Arsenic trioxide or/and copper sulfate co-exposure induce glandular stomach of chicken injury via destruction of the mitochondrial dynamics and activation of apoptosis as well as autophagy. Ecotoxicol. Environ. Saf. 185, 109678.
Park, J., et al., 2018. Long-term occurrence of deoxynivalenol in feed and feed raw materials with a special focus on South Korea. Toxins 10.
Pinton, P., Oswald, I.P., 2014. Effect of deoxynivalenol and other type B trichothecenes on the intestine: a review. Toxins 6, 1615–1643.
Ren, Z., et al., 2020. Effects of deoxynivalenol on mitochondrial dynamics and autophagy in pig spleen lymphocytes. Food Chem. Toxicol. 140, 111357.
Rogers, C., et al., 2017. Cleavage of DFNA5 by caspase-3 during apoptosis mediates progression to secondary necrotic/pyroptotic cell death. Nat. Commun. 8, 14128.
Rotter, B.A., Prelusky, D.B., Pestka, J.J., 1996. Toxicology of deoxynivalenol (vomitoxin). J. Toxicol. Environ. Health 48, 1–34.
Saitoh, T., et al., 2008. Loss of the autophagy protein Atg16L1 enhances endotoxin-induced IL-1beta production. Nature 456, 264–268.
Shi, C.S., et al., 2012. Activation of autophagy by inflammatory signals limits IL-1beta production by targeting ubiquitinated inflammasomes for destruction. Nat. Immunol. 13, 255–263.
Shi, J., et al., 2015. Cleavage of GSDMD by inflammatory caspases determines pyroptotic cell death. Nature 526, 660–665.
Shi, J., Gao, W., Shao, F., 2017. Pyroptosis: gasdermin-mediated programmed necrotic cell death. Trends. Biochem. Sci. 42, 245–254.
Song, J.L., et al., 2022. Deoxynivalenol and zearalenone: different mycotoxins with different toxic effects in donkey (Equus asinus) endometrial epithelial cells. Theriogenology 179, 162–176.
Song, X.B., et al., 2017. Autophagy blockade and lysosomal membrane permeabilization contribute to lead-induced nephrotoxicity in primary rat proximal tubular cells. Cell Death. Dis. 8, e2863.
Sumarah, M.W., 2022. The Deoxynivalenol Challenge. J. Agric. Food Chem. 70, 9619–9624.
Takahama, M., Akira, S., Saitoh, T., 2018. Autophagy limits activation of the inflammasomes. Immunol. Rev. 281, 62–73.
Tang, Y., et al., 2015. Autophagy protects intestinal epithelial cells against deoxynivalenol toxicity by alleviating oxidative stress via IKK signaling pathway. Free Radic. Biol. Med. 89, 944–951.
Thapa, A., et al., 2021. Deoxynivalenol and Zearalenone-synergistic or antagonistic agri-food chain Co-contaminants? Toxins 13.
Wan, S., et al., 2022. Deoxynivalenol damages the intestinal barrier and biota of the broiler chickens. BMC. Vet. Res. 18, 311.
Wang, X., et al., 2020. Autophagy protects PC12 cells against deoxynivalenol toxicity via the class III PI3K/beclin 1/bcl-2 pathway. J. Cell Physiol. 235, 7803–7815.
Wang, Y., et al., 2017. Chemotherapy drugs induce pyroptosis through caspase-3 cleavage of a gasdermin. Nature 547, 99–103.
Wei, Y., et al., 2023. GSDME-mediated pyroptosis promotes the progression and associated inflammation of atherosclerosis. Nat. Commun. 14, 929.
Yang, W., et al., 2019. The effect of low and high dose deoxynivalenol on intestinal morphology, distribution, and expression of inflammatory cytokines of weaning rabbits. Toxins 11.
Yao, Y., Long, M., 2020. The biological detoxification of deoxynivalenol: A review. Food Chem. Toxicol. 145, 111649.
Zhang, Y., et al., 2024. Assessing and mitigating foodborne acetochlor exposure induced ileum toxicity in broiler chicks: the role of omega-3 polyunsaturated fatty acids supplementation and molecular pathways analysis. Pestic. Biochem. Physiol. 199, 105761.
Zingales, V., et al., 2022. Climate change and effects on molds and mycotoxins. Toxins 14.
Zong, Q., et al., 2023. Sodium butyrate ameliorates deoxynivalenol-induced oxidative stress and inflammation in the porcine liver via NR4A2-mediated histone acetylation. J. Agric. Food Chem. 71, 10427–10437.